AD-A170 195 ELASTIC MODULI OF LUNGS REVISION(U) HARVARD UNIV 1/1
CAMBRIDGE MA DIV OF APPLIED SCIENCES
B BUDIANSKY ET AL. OCT 86 MECH-78

UNCLASSIFIED F/G 6/19 NL

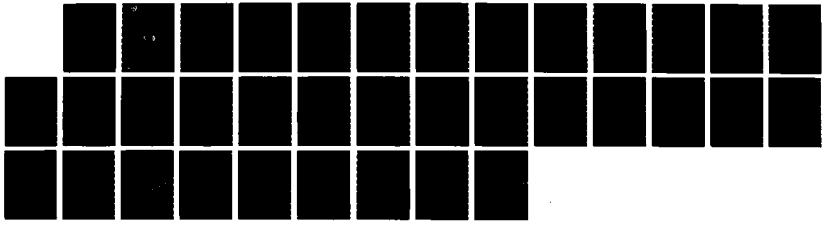

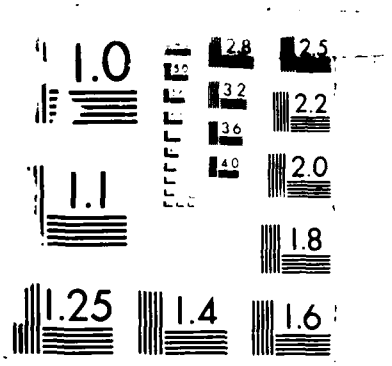
1.0
1.1
1.25
1.4
1.6
1.8
2.0
2.2
2.5
2.8
3.2
3.6
4.0

MECH-78

ELASTIC MODULI OF LUNGS

Bernard Budiansky and Eitan Kimmel

Division of Applied Sciences
HARVARD UNIVERSITY
Cambridge, Massachusetts 02138

May 1986

Revised October 1986

ELASTIC MODULI OF LUNGS

Bernard Budiansky
Division of Applied Sciences
Harvard University
Cambridge, Massachusetts 02138

Eitan Kimmel
Department of Mechanical Engineering
Massachusetts Institute of Technology
Cambridge, Massachusetts 02139

Abstract

Macroscopic elastic moduli governing the incremental deformation of pressurized lungs are calculated on the basis of a micromechanical study of an individual lung element (alveolus). The spongy lung tissue (parenchyma) is presumed to be in an initial state of isotropic tension, and the lung alveolus is idealized as a pin-jointed truss in the shape of a regular dodecahedron. The analysis is based on a variational statement of non-linear structural mechanics, and the results show how the moduli depend on the initial tension and the assumed constitutive behavior of the idealized truss members.

INTRODUCTION

The theory of lung elasticity has received much study during the last two decades, with particular attention directed to the establishment of overall constitutive relations between stress and strain in lung tissue. The most common approach (e.g. Lambert and Wilson, 1973; Frankus and Lee, 1974; Fung et al., 1978; Vawter et al., 1979; Lanir, 1983; Stamenovic and Wilson, 1985) has been to contemplate representative substructural lung elements, idealize their geometries, specify their elastic properties (often via strain-energy functions), assume that local and overall strains are identical, and, finally, get macroscopic constitutive relations by appropriate averages of the local

stresses. The earlier work of Mead et al. (1970) and Wilson (1972) was more in line with the complementary approach of loading representative elements with the macroscopic stress, and computing their strains. In a recent paper, Kimmel et al. (1986) returned to this viewpoint, and studied the elastic behavior of pressurized lungs on the basis of a model in which a typical microstructural element of spongy lung tissue (parenchyma) was idealized as a regular, pin-jointed, dodecahedral space truss (Fig. 1a). An initial isotropic tension transmitted to the parenchyma by the surrounding pressurized pleural membrane was simulated by radial forces at each joint that produced identical tensile forces in the truss members. The model was then used in a calculation of linear, isotropic relations between subsequent small increments of macroscopic stress and strain in the parenchyma. The results showed the dependence of the elastic constants for incremental deformation on the initial hydrostatic tension, and on the tensile constitutive behavior of the idealized truss members. The elastic moduli found were in fairly good agreement with those inferred from available experimental data, but the calculations produced some anomalous results for small values of the stiffness of the element members.

In this paper the model of Kimmel et al. is reformulated, and a rigorous analysis, based on a general variational principle of non-linear structural mechanics, is executed.

MODEL FORMULATION

The microscopic air sacs (alveoli) of which the spongy lung parenchyma is composed are roughly polyhedral in shape, and bounded by thin interfacial membranes. Besides alveoli, the parenchyma is also pervaded by blood vessels, by bronchioles emanating from the main bronchial tubes, by fibers surrounding openings in the alveolar walls, and by fibrous tissues extending from the surrounding pleural membrane (Wilson and Bachofen, 1982). We will pretend that the elastic effects of these extra constituents may be simulated simply by an appropriate thickness of the walls of an alveolar conglomeration. Since each alveolar wall is shared by two alveoli, we will regard the parenchyma as an aggregate of individual hollow polyhedra, the faces of which have *half* the

actual average effective wall thickness. Then, in accordance with standard ideas of composite-material theory, we define the macroscopic strain produced by a prescribed macroscopic stress as the average of the strains experienced by the individual polyhedra in a large piece of parenchyma subjected to boundary tractions consistent with the given stress. When the lung is inflated, the alveolar openings allow the pressures in the alveoli to equalize, so that there are no net pressures across the individual alveolar walls, but a transpulmonary pressure P_0 is applied to the inside surface of the pleura. We will assume that, in turn, the pleural membrane transmits a hydrostatic tension $P < P_0$ to the parenchyma, that this initial hydrostatic stress produces a purely dilatational strain, and that subsequent stress and strain increments are then connected by isotropic constitutive relations.

In this paper, we will bypass the conceptual averaging process needed to determine the macroscopic strain produced by a given stress, and calculate instead the average strain experienced by a *single* hollow element in the shape of a regular dodecahedron. In this analysis, each face of the dodecahedron will be subjected to a traction consistent with the prescribed uniform stress but, at the same time, the surface displacements will be constrained in a way that keeps each face nearly flat. To be precise (see Fig. 1b), it will be assumed that (i) the vector displacement at the center of each pentagonal face is the mean of the displacements at its five corners; and that (ii) on each face the displacement varies linearly within each of the five constituent triangles that meet at the center. Accordingly, the five corner displacements suffice to specify the displacement within each pentagon. It is easily shown that for small displacements satisfying these kinematic assumptions

the average mean curvature of each face vanishes.* By virtue of its symmetry, the isolated dodecahedron, when loaded and constrained in this way, is indeed an elastically isotropic structure, properly reflecting the isotropy of the random aggregate it is meant to represent.

Following Kimmel et al., we make a further simplification, in which we concentrate all of the in-plane load carrying capacity of the dodecahedral faces into elastic, pin-jointed rods along the edges, and adopt for these members the constitutive relation

$$\frac{\dot{T}}{T} = B\left(\frac{\dot{L}}{L}\right) \tag{1}$$

Here T and L are current values of member force and length, dots represent time derivatives, and B is a non-dimensional stiffness that may itself depend on L.

We will first consider a uniform hydrostatic tension P applied normally to the faces of the dodecahedron, and calculate the incremental bulk modulus K defined by

$$K = \dot{P}/(\dot{V}/V) \tag{2}$$

where V is the enclosed volume. Then, with the hydrostatic tension kept constant and normal to the deforming faces, we will apply surface traction rates corresponding to a uniaxial stress σ (Fig. 2) and calculate the Young's modulus

$$E = \dot{\sigma}/\dot{\varepsilon} \tag{3}$$

where $\dot{\varepsilon}$ is the average strain rate in the direction of σ suffered by the dodecahedron. The standard connections for isotropic bodies will then give Poisson's ratio ν and the shear modulus G.

---

* For small deflection $w(x,y)$ normal to an initially flat surface of area A and boundary C, the local mean curvature is

$$\frac{1}{2A}\int_A \nabla^2 w \, dA = \frac{1}{2A}\int_C \frac{\partial w}{\partial n}\, ds$$

where $\partial w/\partial n$ is the normal derivative, and the line integral around the perimeter of the pentagon vanishes when the conditions (i), (ii) are imposed on w.

BULK MODULUS

The calculation of K that follows is essentially the same as that of Kimmel et al. Suppose that hydrostatic tension P produces identical forces T in the 30 members of the dodecahedron. Then, by the principle of virtual work, P produces rates-of-change of volume and length that satisfy

$$P\dot{V} = 30T\dot{L} \tag{4}$$

Self-similar growth of the dodecahedron due to P implies that

$$\dot{V}/V = 3\dot{L}/L \tag{5}$$

so that

$$PV = 10TL \tag{6}$$

and

$$\dot{P}/P + \dot{V}/V = \dot{T}/T + \dot{L}/L \tag{7}$$

Eliminating $\dot{L}/L$ and $\dot{T}/T$ from (5), (7), and (1) gives

$$\dot{P}/P = \left(\frac{B-2}{3}\right)\dot{V}/V$$

and so by the definition (2)

$$K/P = (B-2)/3 \tag{8}$$

YOUNG'S MODULUS

With the hydrostatic tension P maintained, we apply vertical tension σ to the 12 planar faces of the dodecahedron (Fig. 2 shows plan and elevation views of the loaded dodecahedron; geometrical relations are listed in Appendix A). The nominal stress σ is specified as a force per unit horizontal projection of *original* surface area, i.e. the area corresponding to the presence of P alone.

While σ is applied P is kept normal to the *current* surface orientations, and its magnitude in terms of force per unit *current* area is fixed. To begin the analysis of deformation due to σ, we assert the principle of virtual work

$$\sum_{i=1}^{30} T_i \, \delta\Delta_i = P\delta V + \delta\pi \tag{9}$$

where Δ_i represents the elongation of the i^{th} member, T_i is the corresponding force, and π is the potential of the applied σ loading. (The procedure that follows was guided by an earlier development (Budiansky 1969) of equations for the nonlinear analysis of space trusses.) The elongation Δ_i is defined as $(L_i - L_0)$, where L_i is the current member length, and L_0 is the reference length corresponding to the initial state when only P is present. The virtual changes in volume δV and the virtual elongations $\delta\Delta_i$ must be compatible with changes in joint displacements at the corners of the dodecahedron and with the previously stated kinematic assumptions concerning the displacements within the faces of the dodecahedron.

Since there are only three distinct member responses when σ is applied, namely (see Fig. 2) those of (1) AB, (2) BC, and (3) CD, we can replace the internal-virtual-work sum in Eq. (9) by

$$10\sum_{i=1}^{3} T_i \, \Delta_i$$

Also, just four displacement variables suffice to specify the deformation. These are (see Figs. 2, 3) the vertical displacements w_1, w_2 in the direction of the unit vector $\mathbf{k}$ of the joints at A and C, respectively; and the outward displacements v_1, v_2 at B, C, in the horizontal direction $\mathbf{n}_B = \mathbf{n}_C$, pointing away from the vertical central axis of the dodecahedron. The joint displacements elsewhere follow by symmetry.

The $T\delta\Delta$ terms in (9) will be rewritten in terms of the Lagrangian strain defined by

$$\eta = \tfrac{1}{2}(L^2 - L_0^2)/L_0^2$$
$$= \Delta/L_0 + \tfrac{1}{2}(\Delta/L_0)^2 \tag{10}$$

and the modified force variable Q defined as

$$Q \equiv [L_0/(L_0+\Delta)]T \equiv (L_0/L)T \tag{11}$$

It follows that

$$\delta\eta = \delta\Delta/L_0 + \Delta\delta\Delta/L_0^2 = (L/L_0^2)\delta\Delta$$

and

$$T\delta\Delta = L_0 Q \delta\eta$$

so that the variational statement (9) may be transformed to

$$10L_0 \sum_{k=1}^{3} Q_k \delta\eta_k = P\delta V + \delta\pi \tag{12}$$

Note that since $\dot{\eta} = L\dot{L}/L_0^2$, and $\dot{T}/T = \dot{Q}/Q + \dot{L}/L$, the constitutive relation (1) is equivalent to

$$\dot{Q}/Q = (B-1)\dot{L}/L$$

$$= (B-1)(L_0/L)^2 \dot{\eta} \tag{13}$$

The advantage of η over Δ is that it is quadratic instead of irrational in the displacements.

It is convenient to introduce nondimensional displacements y_i (i = 1,2,3,4) defined by

$$[y_1, y_2, y_3, y_4] = [w_1, v_1, w_2, v_2]/L_0 \tag{14}$$

Then, for the three member types, the definition (10) leads to

$$\eta_k = a_{ki}\, y_i + \tfrac{1}{2} b_{kij}\, y_i\, y_j \qquad (k = 1,2,3) \tag{15}$$

in terms of coefficients a_{ki} and $b_{kij} = b_{kji}$ that are derived and listed in Appendix A. Here, and hereafter, we use summation convention, summing from 1 to 4 over repeated subscripts.

The deformed volume V of the dodecahedron can be expressed as a function of the joint displacements by (Appendix B)

$$V = V_0[1 + c_i\, y_i + \tfrac{1}{2} d_{ij}\, y_i\, y_j + O(y^3)] \tag{16}$$

Here V_0 is the original pressurized volume, and $d_{ij} = d_{ji}$. Finally, in Appendix C the potential of the applied tensile stresses is derived in the form

$$\pi = \sigma V_0 [f_i\, y_i] \tag{17}$$

Substituting Eqs. (15)-(17) into Eq. (12) and dividing by PV_0, puts the variational statement of equilibrium into the form

$$\left(\frac{1}{T_0}\right) \sum_{k=1}^{3} Q_k (a_{ki} + b_{kij}\, y_j)\, \delta y_i - [c_i + d_{ij}\, y_j + O(y^2)]\, \delta y_i = (\sigma/P) f_i\, \delta y_i \tag{18}$$

Here we used Eq. (6) to replace $PV_0/(10L_0)$ by T_0.

For $\sigma \to 0$, y_i vanishes and $Q_k \to T_0$, so that (18) becomes

$$\left\{\sum_{k=1}^{3} a_{ki} - c_i\right\} \delta y_i = 0 \tag{19}$$

Since (19) holds for arbitrary variations δy_i, we should have

$$\sum_{k=1}^{3} a_{ki} - c_i = 0 \qquad (i = 1,2,3,4) \tag{20}$$

and it can be verified that these four equations are indeed satisfied. This is consistent with the fact that (19) simply asserts the principle of virtual work at the initial state, and our special assumptions concerning the displacements ensures its validity.

Now we want to use (18) to get a variational statement governing the displacement rates $\dot{y}_i$. Differentiating (18) with respect to time (remembering that the δy_i's are variations that remain arbitrary) gives

$$\left(\frac{1}{T_0}\right) \sum_{k=1}^{3} [\dot{Q}_k (a_{ki} + b_{kij} y_j) + Q_k b_{kij} \dot{y}_j] \delta y_i$$

$$- [d_{ij} \dot{y}_j + O(y\dot{y})] \delta y_i = (\dot{\sigma}/P) f_i \delta y_i \tag{21}$$

Now let $\sigma \to 0$, so that $y_i \to 0$, $L \to L_0$, and $Q_k \to T_0$; then

$$\left\{\frac{1}{T_0} \sum_{k=1}^{3} \dot{Q}_k a_{ki} + \sum_{k=1}^{3} b_{kij} \dot{y}_j - d_{ij} \dot{y}_j\right\} \delta y_i = (\dot{\sigma}/P) f_i \delta y_i \tag{22}$$

Here, by Eq. (13),

$$\dot{Q}_k = T_0 (B-1) \dot{\eta}_k \tag{23}$$

where, by differentiation of Eq. (15), and letting $y_i \to 0$,

$$\dot{\eta}_k = a_{ki} \dot{y}_i \tag{24}$$

Hence (22) implies the four independent equations

$$[(B-1) q_{ij} + s_{ij} - d_{ij}] \dot{y}_j = (\dot{\sigma}/P) f_i \qquad (i = 1,2,3,4) \tag{25}$$

where

$$q_{ij} = \sum_{k=1}^{3} a_{ki} a_{kj} \tag{26}$$

and

$$s_{ij} = \sum_{k=1}^{3} b_{kij} \tag{27}$$

are listed in Appendix B. The dotted quantities in Eqs. (25) now refer to the state at $\sigma = 0$, and these four equations constitute a symmetric system of four simultaneous, linear equations for $\dot{y}_j$ $(j = 1,2,3,4)$. The results will, of course, be proportional to $\dot{\sigma}/P$. Then, to define the average strain rate $\dot{\varepsilon}$, we write

$$\dot{\pi} = \sigma V_0 \dot{\varepsilon} \tag{28}$$

and by Eq. (17) this gives

$$\dot{\varepsilon} = f_i \dot{y}_i \tag{29}$$

The final result for Young's modulus, given by Eq. (3), is

$$E/P = \frac{\dot{\sigma}/P}{(f_i \dot{y}_i)} \tag{30}$$

Thus the solution of Eqs. (25) will provide E/P as a function of B. Then, with the use of Eq. (8) for K/P, the standard relations

$$E = 3K(1-2\nu) = 2G(1+\nu) \tag{31}$$

among Poisson's ratio ν, shear modulus G, E, and K for isotropic materials may be used to compute ν and G/P.

RESULTS AND DISCUSSION

The results for E/P and G/P are plotted versus B in Fig. 4, and Poisson's ratio ν is shown in Fig. 5. It is shown in Appendix D that for $B \to \infty$, the limiting values become

$$\left.\begin{aligned} E/P &= 5(1+\sqrt{5})/4 \\ &= 4.045 \\ G/P &= 1.348 \\ \nu &= 1/2 \end{aligned}\right\} \tag{32}$$

For $B \to 2$, K vanishes, and $\nu \to -1$, because isotropic expansion dominates the strain-rate tensor induced by $\dot{\sigma}$; hence $E/P \sim 9K \sim 3(B-2)$ for $B \to 2$. On the other hand, the shear modulus does not vanish at $B = 2$, where $G/P \approx 1.127$. But for $B < 2$, the structure is unstable, and the values for G/P would not be observable.

The limiting results for $B \to \infty$ shown in (32) are somewhat higher than those of Kimmel et al. (1986), who find $E/P \to 3.51$. But for B less than ~5, the results of Kimmel et al. deviate very markedly from the present ones, showing anomalous *increases* in both E/P and G/P as B decreases. This is probably due to the fact that the various engineering approximations made by Kimmel et al. do not cope adequately with a delicate balance of elastic responses as the instability point at $B = 2$ is approached.

To corroborate the isotropy of our model, an independent computation of Poisson's ratio was made by means of a direct calculation of the average strain-rate tensor in the dodecahedron (Appendix E). An explicit formula (Eq. (E8)) derived for ν in terms of the y_i's was found to provide numerical results in perfect agreement with those calculated from E/P and K/P on the basis of the isotropy relations (31).

We also studied (Appendix F) the effect of imposing an additional constraint on the displacements, keeping each face of the dodecahedron perfectly flat during the imposition of σ. It turns out that for $B \to \infty$, this additional constraint makes no change at all in the limiting results (32). The reason for this is that inextensionality of the members enforces the planarity constraint automatically! Furthermore, the imposition of planarity produced only a tiny increase -- less than 1/10% -- in E/P over the full range $2 < \beta < \infty$, and the results in Figs. 4, 5 were barely changed.

Experiments on dog, pig, and horse lungs by Hajji et al. (1979), involving local external indentation of the pleural membrane of an inflated lung, were used by the investigators to extract values of $G/(1-\nu)$ for incremental straining. Based on the somewhat uncertain value of $P/P_0 = .7$ (Stamenovic and Wilson, 1985, suggest $P/P_0 \sim 3/4$) the results are shown in Fig. 6, where the experimental values of $G/[P(1-\nu)]$ found are compared with the predictions of the present theory. Theory and experiment are generally consistent for the range $B \sim 5$–20, but it should be noted that near the lower end of this range the theoretical values of ν (Fig. 5) become quite low.

CONCLUDING REMARKS

An important feature of the present theoretical approach is that by focusing on incremental stress-strain relations, the constitutive description of the lung substructure has conveniently been thrown into the single elastic parameter B, which, to be sure, may itself depend on the stress level. Not only is B supposed to represent the effective elasticity of a fairly complex structure, it can also be presumed to incorporate the effects of surface tension in the alveolar walls. (That is to say, the basic relation given by Eq. (1) can still be considered to apply, operationally, when surface tension is present.)

The finite limits approached by G/P and E/P for $B \to \infty$ are clearly consequences of the fact that the basic pin-jointed dodecahedron is a statically underdeterminate mechanism (rather than a structure) in the absence of hydrostatic tension. By the same token, it is clear that the use of a statically determinate (or indeterminate) truss model would have led to $G/P, E/P \to \infty$ for $B \to \infty$. Finally, we note that if, in contrast to the present approach, overall properties were calculated via the imposition of a uniform local strain field, then $B \to \infty$ would imply unbounded stiffness for all models -- underdeterminate or not.

ACKNOWLEDGEMENT

This work was supported by a Bantrell Post-Doctoral Fellowship to Eitan Kimmel, the Division of Applied Sciences, Harvard University, and by the Department of Mechanical Engineering, Massachusetts Institute of Technology. Discussions of the theoretical model and of the results were amplified in the light of helpful comments by anonymous reviewers.

REFERENCES

Budiansky, B., 1969, "Remarks on Theories of Solid and Structural Mechanics", Problems of Hydrodynamics and Continuum Mechanics, L. I. Sedov Sixtieth Birthday, SIAM, pp. 77-83.

Frankus, A. and Lee, G. C., 1974, "A Theory of Distortion Studies of Lung Parenchyma Based on Alveolar Membrane Properties", Journal of Biomechanics, Vol. 7, pp. 101-107.

Fung, Y. C. Tong, P, and Patitucci, P., 1978, "Stress and Strain and the Lung", Engineering Mechanics, ASCE Vol. 104, pp. 201-224.

Hajji, M. A., Wilson, T. A. and Lai-Fook, S. J., 1979, "Improved Measurements of Shear Modulus and Pleural Membrane Tension of the Lung", Journal of Applied Physiology: Respiratory and Environmental Exercise Physiology, Vol. 47, pp. 175-181.

Kimmel, E., Kamm, R. D. and Shapiro, A. H., 1986, "A Cellular Model of Lung Elasticity", to be published in the ASME Journal of Biomechanical Engineering.

Lambert, R. K. and Wilson, T. A., 1973, "A Model for the Elastic Properties of the Lung and Their Effect on Expiratory Flow", Journal of Applied Physiology, Vol. 34, pp.34-38.

Lanir, Y., 1983, "Constitutive Equations for the Lung Tissue, ASME Journal of Biomechanical Engineering, Vol. 105, pp. 374-380.

Mead, J., Takishima, T. and Leith, D. , 1970, "Stress Distribution in Lungs: A Model of Pulmonary Elasticity", Journal of Applied Physiology, Vol. 28, pp. 596-608.

Stamenovic, D., Wilson, T. A., 1985, " A Strain Energy Function for Lung Parenchyma", ASME Journal of Biomechanical Engineering, Vol. 107, pp. 81-86.

Vawter, D. L., Fung, Y. C. and West, J. B., 1979, "Constitutive Equation of Lung Tissue Elasticity", ASME Journal of Biomechanical Engineering, Vol. 101 pp. 38-45.

Wilson, T. A., 1972, "A Continuum Analysis of a Two-Dimensional Mechanical Model of the Lung Parenchyma", Journal of Applied Physiology, Vol. 33, pp. 472-478.

Wilson, T. A. and Bachofen, H., 1982, "A Model for the Mechanical Structure of the Alveolar Duct", Journal of Applied Physiology, Vol. 52, pp. 1069-1070.

APPENDIX A

Lagrangian Strains

The geometrical parameters of the regular dodecahedron shown in Fig. 2 satisfy the relations

$$\omega = 54^\circ$$

$$\alpha = 72^\circ$$

$$\sin\omega = \cos\frac{\alpha}{2} = (1+\sqrt{5})/4$$

$$4\sin^2\omega = 1 + 2\sin\omega$$

$$h = \rho_1 = L_0\,(\sec\omega)/2$$

$$\rho_2 = g + h = L_0\tan\omega$$

$$r = L_0\tan\omega\,\sin\omega$$

and the dihedral angle Ω between normals to adjacent planes is

$$\Omega = \arctan 2$$

These relations are useful in the calculations of this Appendix, as well as in those that follow.

Consider a bar PQ having initial length L_0, and let $\mathbf{t}_{PQ}$ represent a unit vector pointing from P to Q. Displacements $\mathbf{U}_P$, $\mathbf{U}_Q$ at P and Q produce the deformed length L_{PQ} satisfying

$$L_{PQ}^2 = \|L_0\mathbf{t} + \mathbf{U}_Q - \mathbf{U}_P\|^2 \tag{A1}$$

The Lagrangian strain (Eq. (10)) is then given by

$$\eta_{PQ} = \frac{\mathbf{t}_{PQ}\cdot(\mathbf{U}_Q - \mathbf{U}_P)}{L_0} + \frac{\|\mathbf{U}_Q - \mathbf{U}_P\|^2}{2L_0^2} \tag{A2}$$

We will now apply the generic relation (A2) to find the strains of members AB, BC, and CD (Fig. 3). The pertinent joint displacements are

$$\left.\begin{aligned}\mathbf{U}_A &= w_1\mathbf{k} + v_1\mathbf{n}_A\\ \mathbf{U}_B &= w_1\mathbf{k} + v_1\mathbf{n}_B\\ \mathbf{U}_C &= w_2\mathbf{k} + v_2\mathbf{n}_C\\ \mathbf{U}_D &= -w_2\mathbf{k} + v_2\mathbf{n}_D\end{aligned}\right\} \tag{A3}$$

Since

$$\mathbf{t}_{AB} \cdot \mathbf{k} = 0 \quad , \quad \mathbf{t}_{AB} \cdot \mathbf{n}_B = -\mathbf{t}_{AB} \cdot \mathbf{n}_A = \cos\,\omega \ ,$$

we get

$$\eta_1 \equiv \eta_{AB} = 2(v_1/L_0)\cos\,\omega + 2(v_1/L_0)^2\cos^2\omega \tag{A4}$$

The unit vector in the direction of CB satisfies

$$\mathbf{t}_{CB} \cdot \mathbf{k} = h/L_0 = (\sec\,\omega)/2$$

$$\mathbf{t}_{CB} \cdot \mathbf{n}_B = \mathbf{t}_{CB} \cdot \mathbf{n}_C = -g/L_0 = -(\csc\,2\omega)/2$$

and so Eq. (A2) gives

$$\eta_2 \equiv \eta_{BC} = \frac{(w_1-w_2)\sec\,\omega}{2L_0} + \frac{(v_2-v_1)\csc\,2\omega}{2L_0} + \frac{(w_1-w_2)^2}{2L_0^2} + \frac{(v_1-v_2)^2}{2L_0^2} \tag{A5}$$

Finally,

$$\mathbf{t}_{DC} \cdot \mathbf{k} = g/L_0 = \tfrac{1}{2}\csc\,2\omega$$

$$\mathbf{t}_{DC} \cdot \mathbf{n}_C = -\mathbf{t}_{DC} \cdot \mathbf{n}_D = (\rho_1/L)\cos\,\alpha = \tfrac{1}{4}\csc\,2\omega$$

and with $\|\mathbf{n}_C - \mathbf{n}_D\|^2 = 2(1-\sin\,\omega)$, Eq. (A2) produces

$$\eta_3 \equiv \eta_{CD} = (w_2/L_0)\csc\,2\omega + \tfrac{1}{2}(v_2/L_0)\csc\,2\omega + 2(w_2/L_0)^2 + (1-\sin\,\omega)(v_2/L_0)^2 \tag{A6}$$

Rewritten in terms of the y_i's (Eq. (14)), Eqs. (A4)–(A6) provide the following results for the coefficients a_{ki} in (15):

$$[a_{ki}] = \frac{1}{2}\begin{bmatrix} 0 & 4\cos\,\omega & 0 & 0 \\ \sec\,\omega & -\csc\,2\omega & -\sec\,\omega & \csc\,2\omega \\ 0 & 0 & 2\csc\,2\omega & \csc\,2\omega \end{bmatrix} \tag{A7}$$

The coefficients b_{1ij} vanish, except for

$$b_{122} = 4\cos^2\omega \tag{A8}$$

The matrix of coefficients b_{2ij} is

$$[b_{2ij}] = \begin{bmatrix} 1 & 0 & -1 & 0 \\ 0 & 1 & 0 & -1 \\ -1 & 0 & 1 & 0 \\ 0 & -1 & 0 & 1 \end{bmatrix} \tag{A9}$$

Finally, the only b_{3ij} that do not vanish are

$$b_{333} = 4$$
$$b_{344} = 2(1\text{-}\sin\omega) \tag{A10}$$

The coefficients q_{ij} and s_{ij} defined by Eqs. (26) and (27) are

$$q_{ij} = \left(\frac{\sec^2\omega}{4}\right) \begin{bmatrix} 1 & -(\csc\omega)/2 & -1 & (\csc\omega)/2 \\ -(\csc\omega)/2 & 3(\csc^2\omega)/2 & (\csc\omega)/2 & -(\csc^2\omega)/4 \\ -1 & (\csc\omega)/2 & 9-8\sin\omega & (\csc^4\omega)/16 \\ (\csc\omega)/2 & -(\csc^2\omega)/4 & (\csc^4\omega)/16 & (\csc^2\omega)/2 \end{bmatrix} \tag{A11}$$

and

$$[s_{ij}] = \begin{bmatrix} 1 & 0 & -1 & 0 \\ 0 & 4-2\sin\omega & 0 & -1 \\ -1 & 0 & 5 & 0 \\ 0 & -1 & 0 & 3-2\sin\omega \end{bmatrix} \tag{A12}$$

APPENDIX B

Volume Change

Together with the assumptions made concerning the piecewise linear displacement patterns within each face, the corner displacements w_1, v_1, w_2, v_2 (Fig. 3) determine the configuration of the dodecahedron subjected to uniform tension. The deformed volume can be written as (Fig. 1b)

$$V = 2V_{ABFGH} + 10[V_{AXB} + 2V_{BXC} + 2V_{CXD}] \tag{B1}$$

wherein each of the subscripted terms represents the volume of a pyramid with its apex at the center of the dodecahedron, and the subscript denotes the base. The *original* area of the pentagon ABFGH was

$$A_0 = (5/4) L_0^2 \tan \omega \tag{B2}$$

and the altitude of the corresponding pyramid was (Fig. 2)

$$r = L_0 \tan \omega \sin \omega$$

Hence the deformed volume is

$$V_{ABFGH} = 5(L_0 \tan \omega \sin \omega + w_1)(L_0 + 2v_1 \cos \omega)^2 \tan \omega/12 \tag{B3}$$

To facilitate the calculation of the remaining terms in (B1), we use the orthogonal unit vectors (**i**,**j**,**k**) shown in Fig. 2 to write the original position vectors of A, B, C, D, E and X as

$$\left.\begin{aligned} \mathbf{A}, \mathbf{B} &= [\pm \mathbf{i}/2 + \mathbf{j}(\tan \omega)/2 + \mathbf{k} \tan \omega \sin \omega] L_0 \\ \mathbf{C}, \mathbf{E} &= [\mp \mathbf{i} \sin \omega + \mathbf{j} \tan \omega \sin \omega + \mathbf{k} (\csc 2\omega)/4] L_0 \\ \mathbf{D} &= [\mathbf{j} \tan \omega - \mathbf{k} (\csc 2\omega)/4] L_0 \\ \mathbf{X} &= [2\mathbf{j} + \mathbf{k}][\tan \omega (1 + \sin \omega)]/5 \end{aligned}\right\} \tag{B4}$$

The displacement vectors are

$$\left.\begin{aligned} \mathbf{w}_A, \mathbf{w}_B &= \pm \mathbf{i}\, v_1 \cos\omega + \mathbf{j} v_1 \sin\omega + \mathbf{k} w_1 \\ \mathbf{w}_C, \mathbf{w}_E &= \mp \mathbf{i}\, v_2 \cos\omega + \mathbf{j} v_2 \sin\omega + \mathbf{k} w_2 \\ \mathbf{w}_D &= \mathbf{j} v_2 - \mathbf{k} w_2 \\ \mathbf{w}_X &= [\mathbf{w}_A + \mathbf{w}_B + \mathbf{w}_C + \mathbf{w}_D + \mathbf{w}_E]/5 \\ &= \mathbf{j}[2v_1 \sin\omega + v_2(1 + 2\sin\omega)]/5 + \mathbf{k}[2w_1 + w_2]/5 \end{aligned}\right\} \quad \text{(B5)}$$

Then

$$V_{ABX} = [\mathbf{A} + \mathbf{w}_A] \times [\mathbf{X} + \mathbf{w}_X] \cdot [\mathbf{B} + \mathbf{w}_B]/6 \quad \text{(B6)}$$

and similarly for the remaining two pyramidal volumes in (B1). Carrying out the required straightforward but tedious calculations leads to

$$\begin{aligned} V = V_0 &+ [w_1(3 + 8\sin\omega)/2 + 2v_1(1 + \sin\omega) + w_2(-1 + 4\sin\omega)/2 \\ &+ v_2(1 + 6\sin\omega)]L_0^2 \tan\omega \\ &+ [v_1^2(2 + \sin\omega) + v_2^2(2 + 3\sin\omega) + 2w_1 v_1(3 + 2\sin\omega) \\ &+ w_1 v_2(7 + 6\sin\omega) - 4w_2 v_1 + 4v_1 v_2 \sin\omega \\ &+ w_2 v_2(5 + 2\sin\omega)][2L_0 \sin\omega]/3 \\ &+ [\text{cubic terms}] \end{aligned}$$

where the original volume V_0 is

$$V_0 = 5L_0^3 \tan^2\omega \sin\omega \quad \text{(B7)}$$

The coefficients in the expansion in (16) for V/V_0 in terms of the nondimensional y's are then

$$\left.\begin{aligned} c_1 &= \cot\omega(3\csc + 8)/10 \\ c_2 &= 2\cot\omega(\csc + 1)/5 \\ c_3 &= \cot\omega(-\csc + 4)/10 \\ c_4 &= \cot\omega(\csc + 6)/5 \end{aligned}\right\} \quad \text{(B8)}$$

and

$$[d_{ij}] = (2\cot^2\omega/15)\begin{bmatrix} 0 & 6+4\sin\omega & 0 & 7+6\sin\omega \\ 6+4\sin\omega & 2(2+\sin\omega) & -4 & 4\sin\omega \\ 0 & -4 & 0 & 5+2\sin\omega \\ 7+6\sin\omega & 4\sin\omega & 5+2\sin\omega & 2(2+3\sin\omega) \end{bmatrix} \quad \text{(B9)}$$

APPENDIX C

Stress Potential

If the applied σ stresses in the **k** direction produce the surface displacements **u**, then the potential of the stresses is

$$\pi = \int_S [\mathbf{n} \cdot \sigma\mathbf{k}\mathbf{k} \cdot \mathbf{u}]dS \tag{C1}$$

where the integration is over the undeformed surface, and **n** is the unit normal to this surface. Our kinematic assumptions imply that (Fig. 1b) the face ABFGH remains plane, as does its counterpart at the bottom of the dodecahedron. Hence the partial potential of the σ-stresses applied to these two faces is simply

$$[2\sigma A_0 w_1] \tag{C2}$$

where A_0 is the original area of the pentagon.

In face ABCDE (Fig. 1b), the midpoint vector displacement $\mathbf{w}_X$ is the mean of the five corner displacements, the average over each triangle of the linearly varying displacements within each triangle is the mean of its three corner displacements, and it follows that the average displacement over the pentagon is also $\mathbf{w}_X$. Hence the potential of the σ-stresses is just

$$(\mathbf{n} \cdot \sigma\mathbf{k}\mathbf{k} \cdot \mathbf{w}_X)A_0 \tag{C3}$$

But (Fig. 3)

$$\mathbf{w}_X \cdot \mathbf{k} = (2w_1 + w_2)/5 \tag{C4}$$

$$\mathbf{n} \cdot \mathbf{k} = \cos\,\Omega = 1/\sqrt{5} \tag{C5}$$

and the contribution (C3) is

$$\sigma A_0 \cos\,\Omega\,(2w_1 + w_2)/5 \tag{C6}$$

Adding 10 such contributions to (C2) gives the total potential

$$\pi = 2\sigma A_0[(1 + 2\cos\,\Omega)w_1 + w_2 \cos\,\Omega]$$

$$= 2\sigma A_0[(1 + 2/\sqrt{5})w_1 + w_2/\sqrt{5}] \tag{C7}$$

Hence, with the use of Eqs. (B2) and (B7) for A_0 and V_0, which give

$$A_0 L_0 / V_0 = (\cot \omega \csc \omega)/4 \tag{C8}$$

the coefficients f_i in Eq. (17) become

$$\left.\begin{aligned} f_1 &= (\cot \omega)(\csc \omega)(1 + 2/\sqrt{5})/2 \\ f_2 &= 0 \\ f_3 &= (\cot \omega)(\csc \omega)/(2\sqrt{5}) \\ f_4 &= 0 \end{aligned}\right\} \tag{C9}$$

APPENDIX D

Inextensional Limit, $B \to \infty$

For $B \to \infty$, the members become inextensional, and therefore the strain rates given by Eq.(24) must vanish:

$$a_{ki}\, \dot{y}_i = 0 \qquad (k = 1,2,3) \tag{D1}$$

It follows that for $B \to \infty$,

$$\dot{y}_i = \beta_i c \tag{D2}$$

where, in accordance with the a_{ki} matrix shown in (A7),

$$\beta_1 = \sqrt{5}\ ,\ \beta_2 = 0\ ,\ \beta_3 = 1\ ,\ \beta_4 = -2 \tag{D3}$$

To evaluate the constant c, substitute (D2) into the variational statement (22) and choose $\delta y_i = \beta_i$. This gives

$$c[s_{ij} - d_{ij}]\beta_i \beta_j = (\dot{\sigma}/P) f_i \beta_i \tag{D4}$$

and then the limiting value of *E/P, from Eq. (30), becomes*

$$E/P = (s_{ij} - d_{ij})\beta_i \beta_j /(f_k \beta_k)^2 \tag{D5}$$

Substitution of the values of s_{ij}, d_{ij}, and f_k given in Eqs. (A12), (B9), and (C9), respectively, provides the result (after considerable reduction)

$$E/P = 5 \sin \omega$$

$$= 5(1 + \sqrt{5})/4 \tag{D6}$$

and this was corroborated numerically via the solution of Eqs. (25) for very large B.

APPENDIX E

Average Strain Rates

The average strain-rate tensor $\dot{\boldsymbol{\varepsilon}}$ in a body V_0 that suffers velocities $\mathbf{u}$ on its boundary S is

$$\dot{\boldsymbol{\varepsilon}} = \left\{ \int_S (\dot{\mathbf{u}}\mathbf{n} + \mathbf{n}\dot{\mathbf{u}})\,dS \right\} /(2V_0) \tag{E1}$$

where $\mathbf{n}$ is the unit normal to S. If we let $\dot{\varepsilon} = \mathbf{k}\cdot\dot{\boldsymbol{\varepsilon}}\cdot\mathbf{k}$ denote the strain rate in the $\mathbf{k}$ direction, (E1) gives

$$\dot{\varepsilon} = \left\{ \int_S (\mathbf{k}\cdot\dot{\mathbf{u}})(\mathbf{n}\cdot\mathbf{k})\,dS \right\} /V_0 \tag{E2}$$

which, by (C1), is the same as $\dot{\pi}/(V_0\sigma) = f_i\dot{y}_i$. Hence, direct averaging to calculate E/P gives the same result as that found from the use of the energy definition (28) for $\dot{\varepsilon}$. However, an independent calculation of Poisson's ratio can be based on the direct calculation of the mean transverse strain rate

$$\dot{\varepsilon}_T \equiv (\mathbf{i}\cdot\dot{\boldsymbol{\varepsilon}}\cdot\mathbf{i} + \mathbf{j}\cdot\dot{\boldsymbol{\varepsilon}}\cdot\mathbf{j})/2 \tag{E3}$$

Since $\mathbf{n}\cdot\mathbf{i} = 0$ on ABCDE (see Fig. 2)

$$\dot{\varepsilon}_T = 10\left\{ \int_{ABCDE} (\mathbf{n}\cdot\mathbf{j})(\dot{\mathbf{u}}\cdot\mathbf{j})\,dS \right\} /(2V_0) \tag{E4}$$

But

$$\mathbf{n}\cdot\mathbf{j} = \sin\,\Omega = 2/\sqrt{5} \tag{E5}$$

and

$$\int_{ABCDE} (\dot{\mathbf{u}}\cdot\mathbf{j})\,dS = (\dot{\mathbf{w}}_X\cdot\mathbf{j})\,A_0$$

$$= [2\dot{v}_1 \sin\,\omega + \dot{v}_2\,(1 + \sin\,\omega)]A_0/5 \tag{E6}$$

where (B5) has been used for $\mathbf{w}_X$. Hence (E4) gives

$$\dot{\varepsilon}_T = 2[2\dot{y}_2 \sin\,\omega + \dot{y}_4(1 + 2\sin\,\omega)][A_0L_0]/(V_0\sqrt{5})$$

$$= [\dot{y}_2(1 + \sqrt{5}) + \dot{y}_4(3 + \sqrt{5})][\cot\,\omega\,\csc\,\omega]/(4\sqrt{5}) \tag{E7}$$

Since $\dot{\varepsilon}_T = -\nu\dot{e} = -\nu f_i \dot{y}_i$ we find, with Eq. (C8) for f_i,

$$\nu = -\frac{1}{2}\left[\frac{\dot{y}_2(1+\sqrt{5}) + \dot{y}_4(3+\sqrt{5})}{\dot{y}_1(2+\sqrt{5}) + \dot{y}_3}\right] \tag{E8}$$

APPENDIX F

Planarity Constraint

An edge view of the pentagon ABCDE (Fig. 3) is shown in Fig. 7. For the corners of the displaced pentagon A'B'C'D'E' to remain co-planar, we must have

$$\frac{h + w_1 - w_2}{h/2 + (v_2 - v_1)\sin\omega} = \frac{g + 2w_2}{g/2 + v_2(1 - \sin\omega)} \tag{F1}$$

In terms of the non-dimensional displacements y_i, this reduces to the condition

$$F \equiv g_i y_i + \tfrac{1}{2} h_{ij} y_i y_j = 0 \tag{F2}$$

where

$$\left.\begin{aligned} g_1 &= (\sec\omega)/2 \\ g_2 &= \tan\omega \\ g_3 &= -(\sec\omega)/2 - 2\tan\omega \\ g_4 &= -(\sec\omega)/2 \end{aligned}\right\} \tag{F3}$$

$$\left.\begin{aligned} h_{14} = h_{41} &= -1 + 2\sin\omega \\ h_{23} = h_{32} &= 2(1 + 2\sin\omega) \\ h_{34} = h_{43} &= -(1 + 6\sin\omega) \end{aligned}\right\} \tag{F4}$$

and all other h_{ij}'s vanish.

To impose the constraint (F2), we introduce the scalar Lagrangian multiplier λ, and add

$$\lambda\delta F \equiv \lambda(g_i + h_{ij} y_j)\delta y_i \tag{F5}$$

to the left side of the variational statement (18). It follows from this modified variational equation that if $\lambda \to \lambda_0$ for $\sigma \to 0$, then

$$\left\{\sum_{k=1}^{3} a_{ki} - c_i + \lambda_0 g_i\right\}\delta y_i = 0 \tag{F6}$$

and therefore (Eq. (20)) $\lambda_0 = 0$. If we now reproduce the steps that originally led to Eq. (25), the corresponding equations for the constrained problem become

$$[(B-1)q_{ij} + s_{ij} - d_{ij}]\,\dot{y}_j + \dot{\lambda}\, g_i = (\dot{\sigma}/P) f_i \qquad (i = 1,2,3,4) \qquad \text{(F7)}$$

where $\dot{\lambda}$ refers to the state at $\sigma = 0$. These four equations, together with the differentiated constraint relation

$$g_i\, \dot{y}_i = 0 \qquad \text{(F8)}$$

that holds for $y_i = 0$, constitute a symmetric system of five linear equations for $\dot{y}_1$, $\dot{y}_2$, $\dot{y}_3$, $\dot{y}_4$ and $\dot{\lambda}$, and their numerical solution provided the results discussed in the text. The equations of inextensionality (D1) and the planarity condition (F8) are equivalent to the homogeneous relations

$$\begin{bmatrix} 0 & 1 & 0 & 0 \\ 2\sin\omega & -1 & -2\sin\omega & 1 \\ 0 & 0 & 2 & 1 \\ 1 & 2\sin\omega & -1-4\sin\omega & -1 \end{bmatrix} \begin{bmatrix} \dot{y}_1 \\ \dot{y}_2 \\ \dot{y}_3 \\ \dot{y}_4 \end{bmatrix} = 0 \qquad \text{(F9)}$$

Remarkably, the matrix of coefficients is singular, so that the limiting solution (D2), (D3) for $\dot{y}_i$ in the limit $B \to \infty$ remains valid, as do the limiting results for the moduli. Thus, planarity, at least for small displacements, is a consequence of inextensionality.

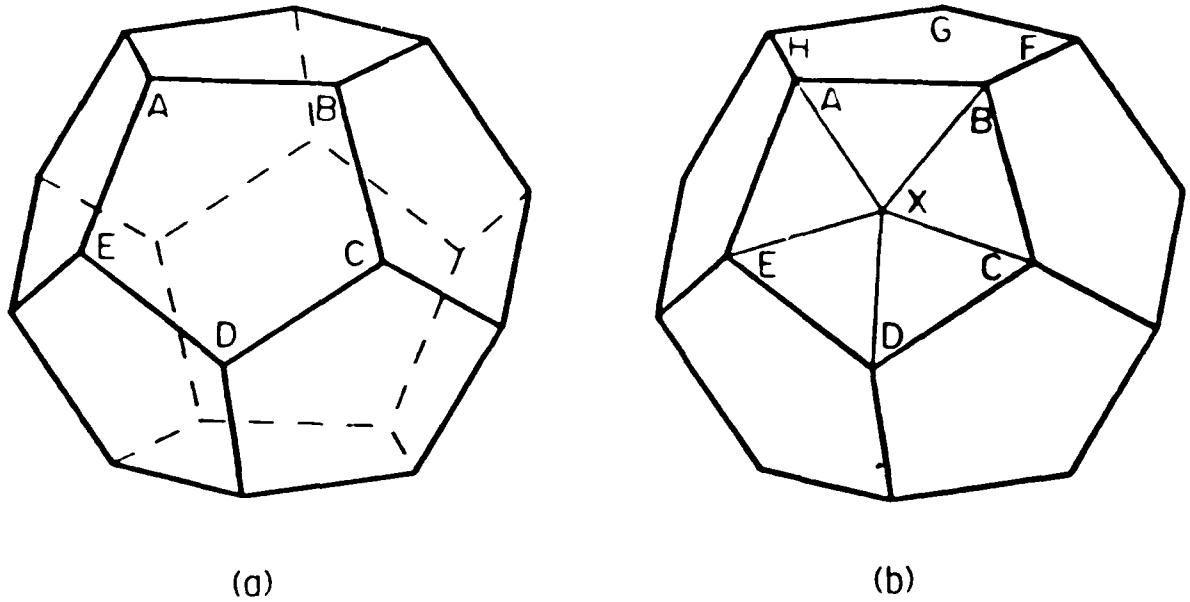

Fig. 1 (a) Regular dodecahedron, (b) subdivision of pentagonal faces.

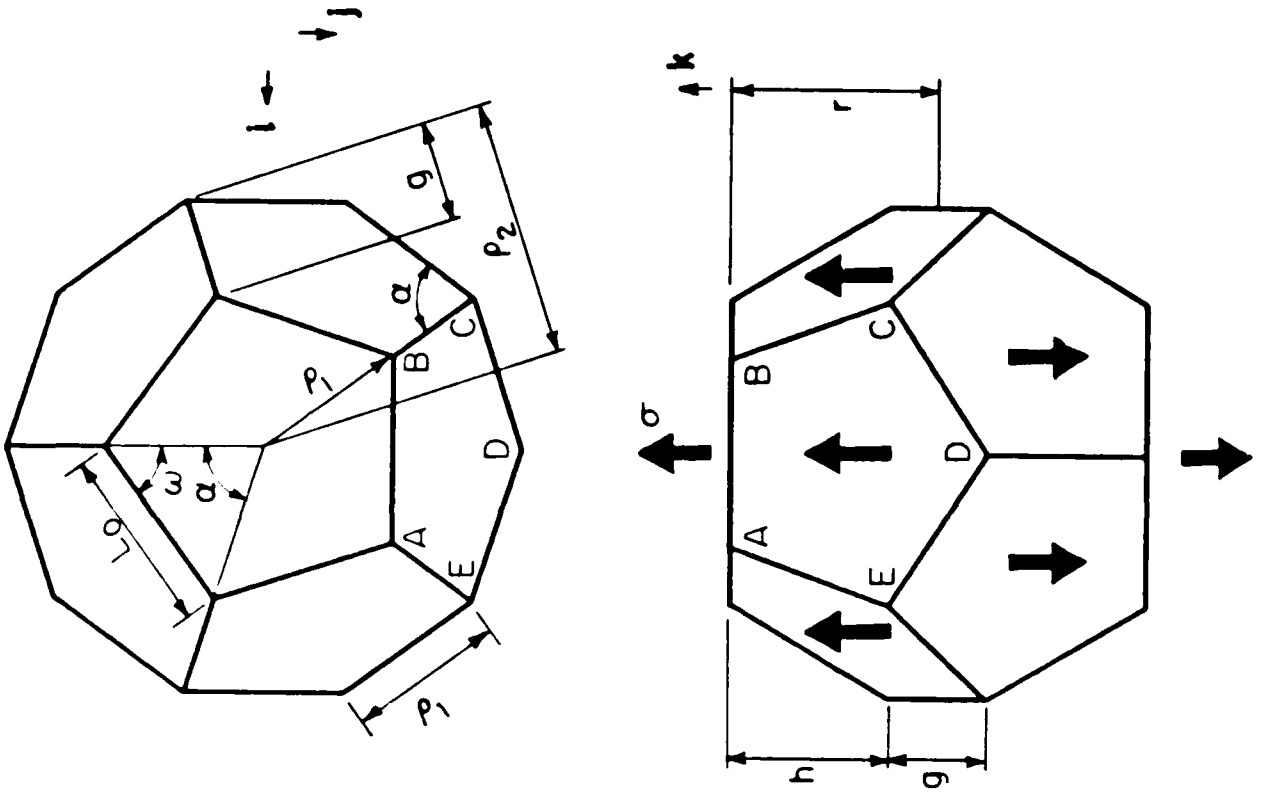

Fig. 2 Plan and elevation views; notation.

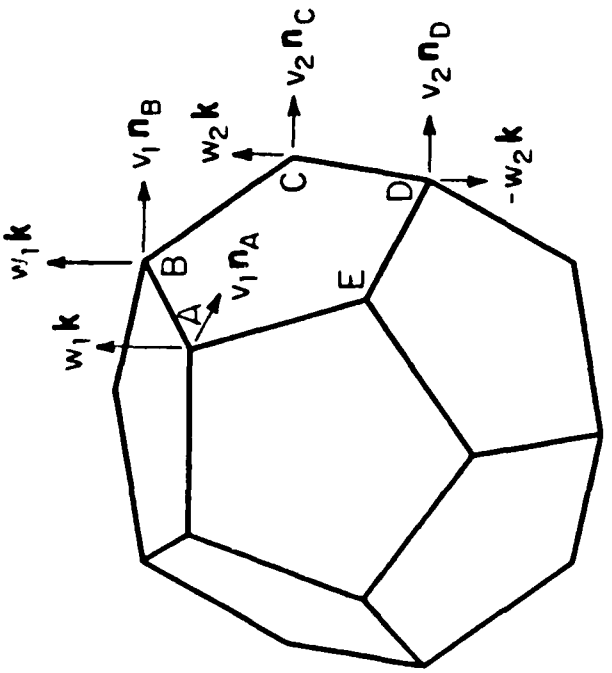

Fig. 3 Corner displacements produced by uniaxial tension.

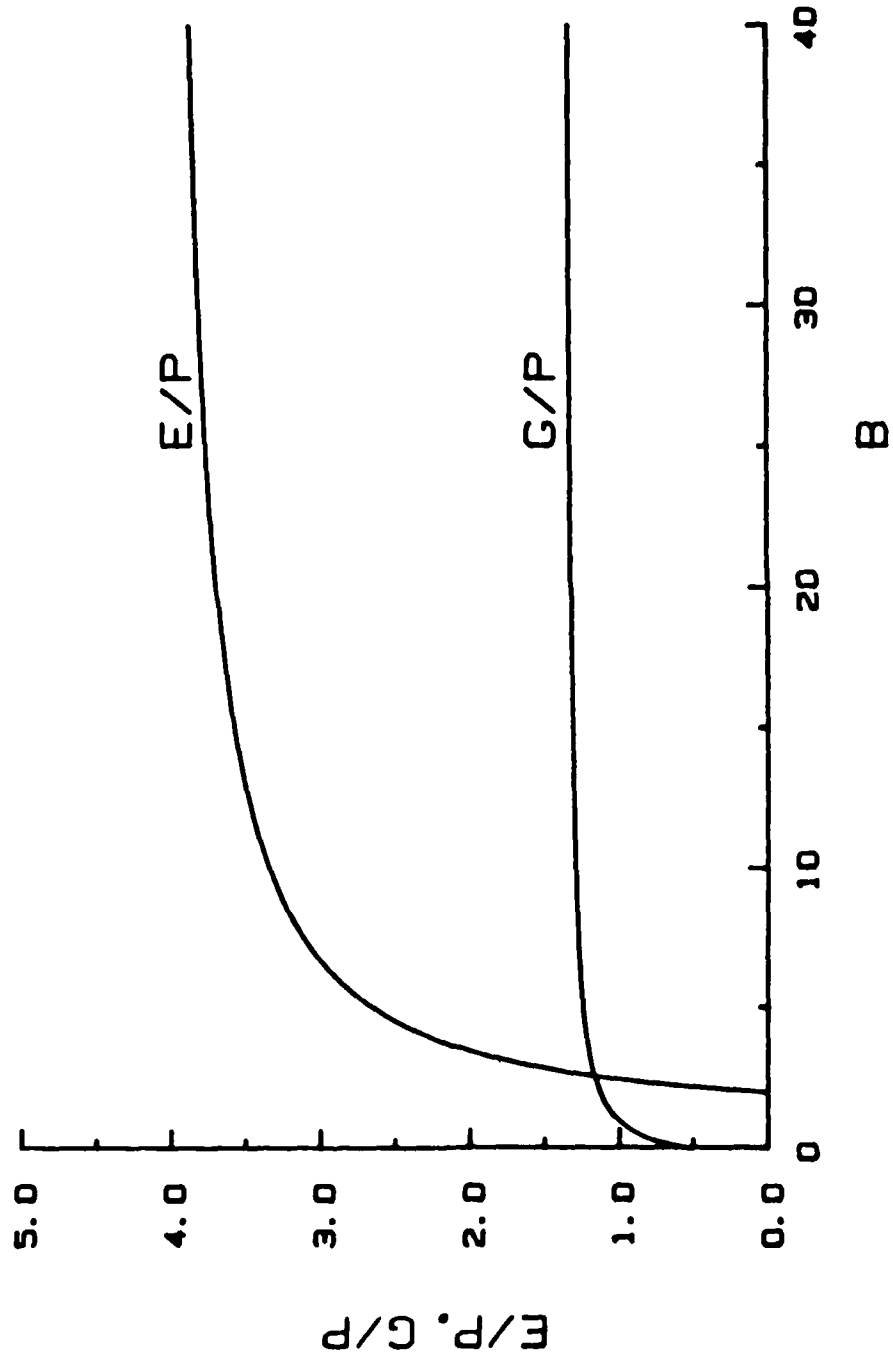

Fig. 4 Normalized Young's modulus E and shear modulus G.

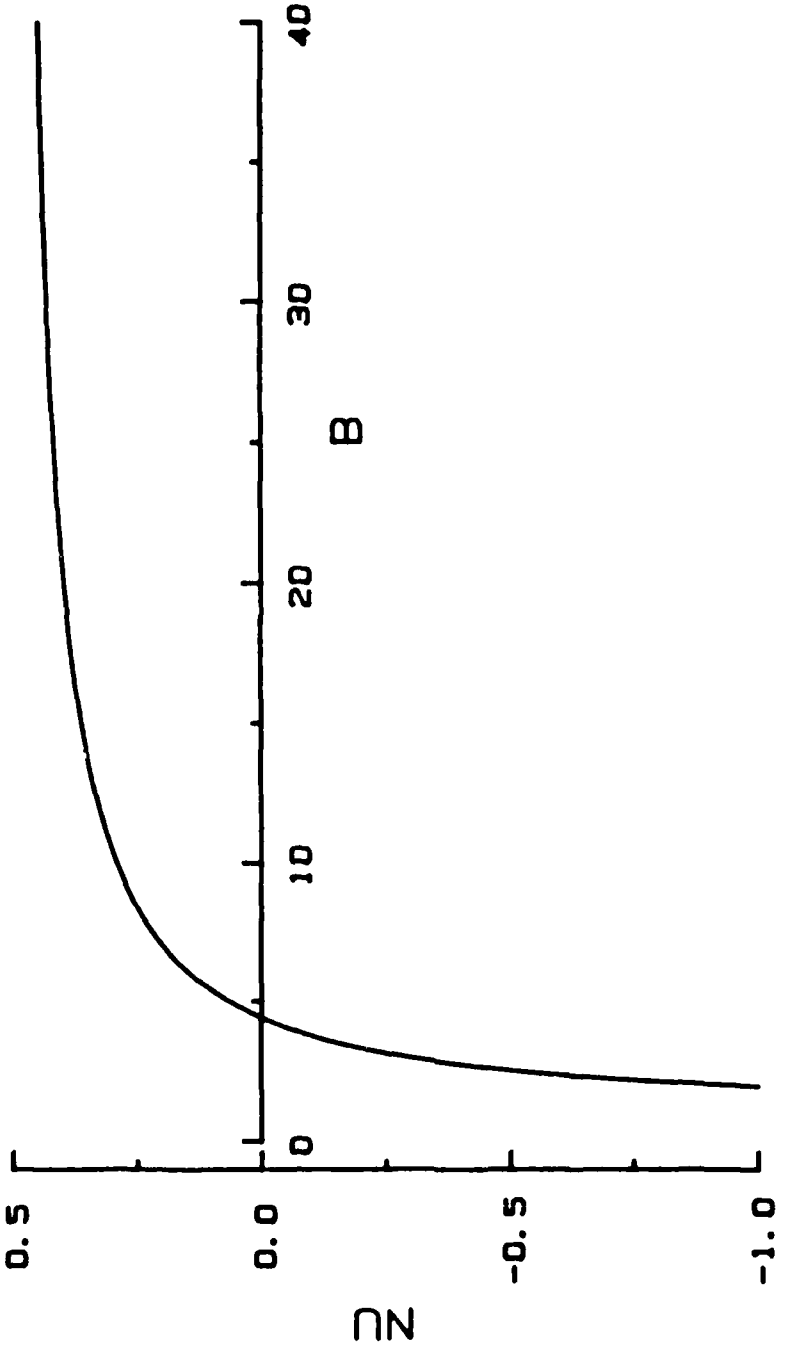

Fig. 5 Poisson's ratio ν.

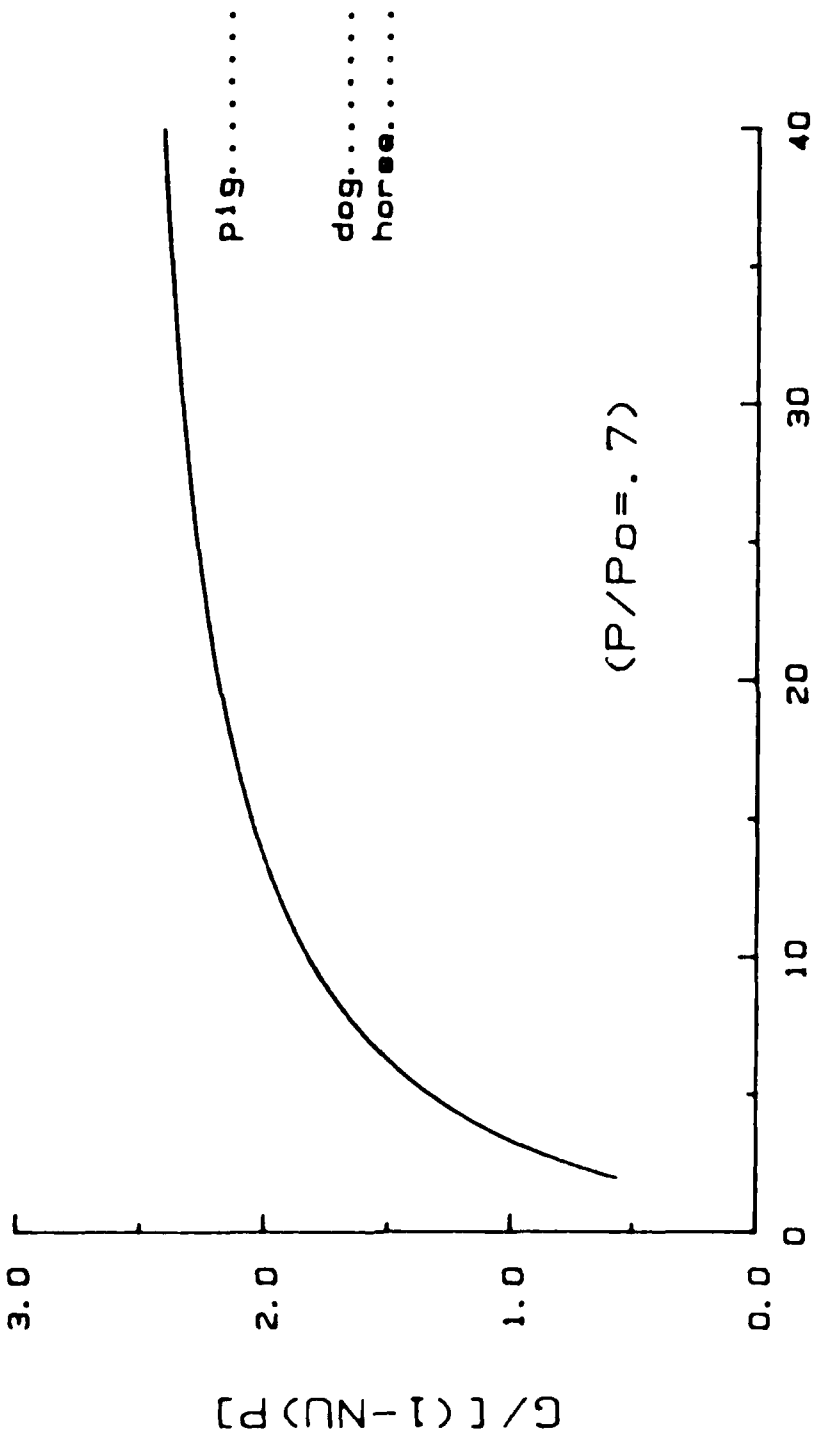

Fig. 6 Comparison of theory and experiment.

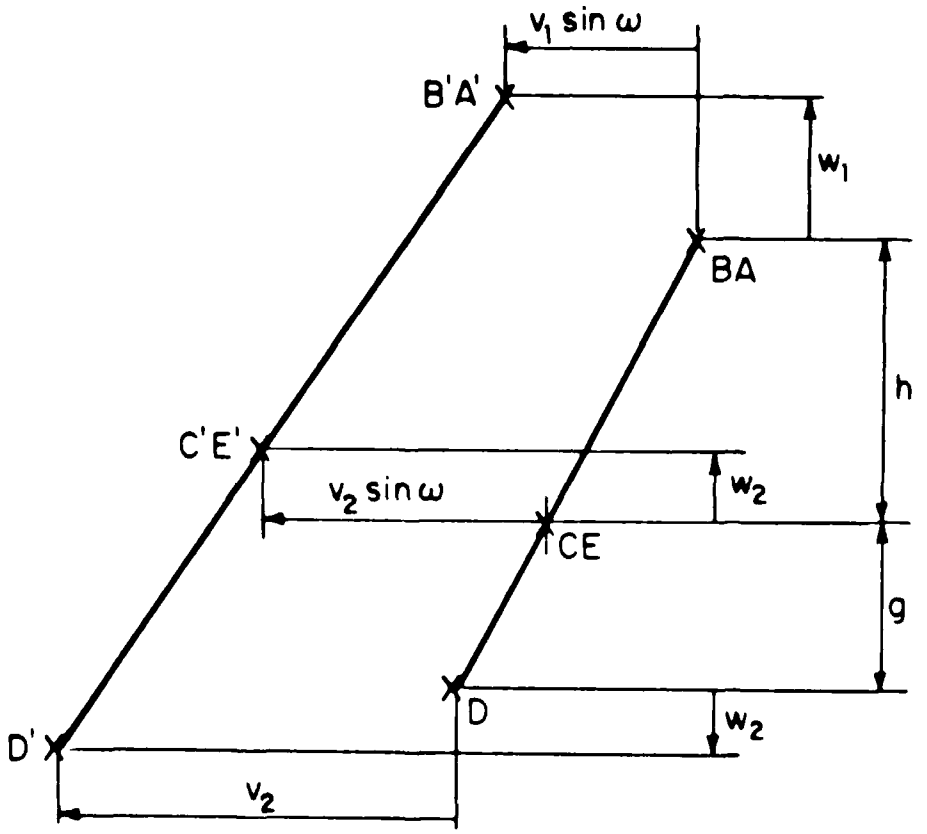

Fig. 7 Corner displacements constrained by planarity condition.

END

5-87

DTIC